PHYSICAL REVIEW B **79**, 041302(R) (2009)

Strong magnetic coupling between an electronic spin qubit and a mechanical resonator

P. Rabl,[1,2] P. Cappellaro,[1,2] M. V. Gurudev Dutt,[3] L. Jiang,[2] J. R. Maze,[2] and M. D. Lukin[1,2]
[1]*ITAMP, Harvard-Smithsonian Center for Astrophysics, Cambridge, Massachusetts 02138, USA*
[2]*Department of Physics, Harvard University, Cambridge, Massachusetts 02138, USA*
[3]*Department of Physics and Astronomy, University of Pittsburgh, Pittsburgh, Pennsylvania 15260, USA*
(Received 18 November 2008; published 8 January 2009)

We describe a technique that enables a strong coherent coupling between a single electronic spin qubit associated with a nitrogen-vacancy impurity in diamond and the quantized motion of a magnetized nanomechanical resonator tip. This coupling is achieved via careful preparation of dressed spin states which are highly sensitive to the motion of the resonator but insensitive to perturbations from the nuclear-spin bath. In combination with optical pumping techniques, the coherent exchange between spin and motional excitations enables ground-state cooling and controlled generation of arbitrary quantum superpositions of resonator states. Optical spin readout techniques provide a general measurement toolbox for the resonator with quantum limited precision.

DOI: 10.1103/PhysRevB.79.041302 PACS number(s): 71.55.−i, 07.10.Cm, 42.50.Pq

I. INTRODUCTION

Techniques for cooling and quantum manipulation of motional states of nanomechanical resonators are now actively explored. Work in this field is motivated by ideas from quantum information science,[1,2] testing quantum mechanics for macroscopic objects,[3,4] and potential applications in nanoscale sensing.[5,6] Approaches based on mechanical resonators coupled to optical cavities,[7] superconducting devices,[8,9] or cold atoms[10] are presently being investigated in experiments.

This Rapid Communication describes a technique that enables a coherent coupling between the quantized motion of a mechanical resonator and an isolated spin qubit. Specifically, we focus on the electronic spin associated with a nitrogen-vacancy (NV) impurity in diamond[11] which can be optically polarized and detected and exhibits excellent coherence properties even at room temperature.[12] Since its precession frequency depends on external magnetic fields via the Zeeman effect, single spins can be used as magnetic sensors operating at nanometer scales.[13,14]

The essential idea of the present work can be understood by considering a prototype system shown in Fig. 1. Here a single spin is used to sense the motion of the magnetized resonator tip that is separated from the spin by an average distance h and oscillates at frequency ω_r. These oscillations produce a time-varying magnetic field that causes Zeeman shifts of the spin qubit. Specifically, the shift corresponding to a single quantum of motion is $\lambda = g_s \mu_B G_m a_0$, where $g_s \simeq 2$, μ_B is the Bohr magneton, G_m is the magnetic field gradient, and $a_0 = \sqrt{\hbar/2m\omega_r}$ is the amplitude of zero-point fluctuations for a resonator of mass m. For realistic conditions $h \approx 25$ nm, $\omega_r/2\pi \approx 5$ MHz, $a_0 \approx 5 \times 10^{-13}$ m, and $G_m \approx 10^7$ T/m, we find that $\lambda/2\pi$ can approach 100 kHz. Such a large shift can be easily measured within a fraction of a millisecond by detecting the electronic spin state.[14] More importantly, the coupling constant λ can considerably exceed both the electronic spin coherence time ($T_2 \sim 1$ ms) and the intrinsic damping rate, $\gamma = \omega_r/Q$, of high-Q mechanical resonators. In this regime, the spin becomes strongly coupled to mechanical motion in direct analogy to strong coupling of cavity quantum electrodynamics.

Before proceeding we note that coupling of mechanical motion to several types of matter qubits, ranging from Cooper pair boxes to trapped atoms, has been considered previously.[3,10,15] The distinguishing feature of the present approach is that working at nanoscale dimensions allows us to combine a well-isolated spin qubit with a large interaction strength, thus enabling the strong-coupling regime. In what follows we describe how this regime can be accessed in the presence of fast dephasing ($T_2^* \sim 1$ μs) of the electronic spin due to interactions with the nuclear-spin bath by using an appropriate dressed spin basis. We then show how it can be applied to cooling and quantum manipulation of mechanical motion.

In the setup shown in Fig. 1 the nanomechanical resonator is described by the Hamiltonian $H_r = \hbar\omega_r a^\dagger a$, with ω_r as the frequency of the fundamental bending mode and a and $a^\dagger$ as the corresponding annihilation and creation operators. Motion of the magnetic tip produces a field $|\vec{B}_{\rm tip}| \simeq G_m \hat{z}$, which is proportional to the position operator $\hat{z} = a_0(a + a^\dagger)$ and results in a Hamiltonian,

$$H_S = H_{\rm NV} + \hbar\omega_r a^\dagger a + \hbar\lambda(a + a^\dagger)S_z. \tag{1}$$

Here $H_{\rm NV}$ describes the dynamics of the driven electronic spin and S_z is the z component of the spin operator which we here assume to be aligned with the NV symmetry axis.

The electronic ground state of the NV center is an $S=1$ spin triplet, and we label states by $|m_s\rangle$, where $m_s = 0, \pm 1$.

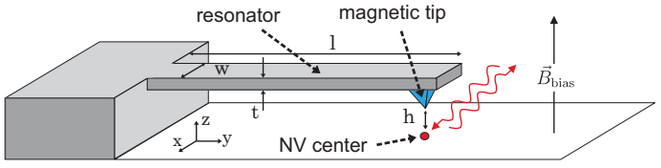

FIG. 1. (Color online) The magnetic tip attached to the end of a nanomechanical resonator of dimensions (l,w,t) is positioned at a distance $h \sim 25$ nm above a single NV center, thereby creating a strong coupling between the electronic spin of the defect center and the motion of the resonator. Microwave and laser fields are used to manipulate and measure the spin states.

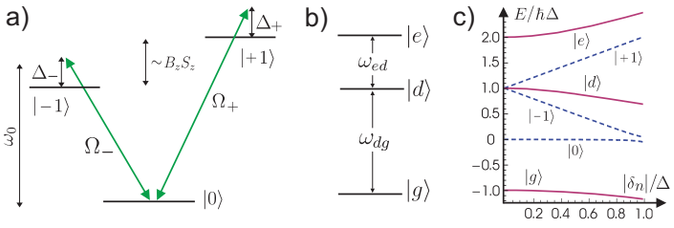

FIG. 2. (Color online) (a) Level diagram of the driven NV center in the electronic ground state. (b) Dressed spin basis states for $\Omega \sim |\Delta|$ and $\Delta < 0$. (c) Energies of dressed states in the presence of external perturbations of the form $H_{\rm nuc} = \hbar \delta_n S_z$ for $\Omega/|\Delta| = 0.1$ (dashed line) and $\Omega/|\Delta| = 1$ (solid line).

Spin states with different values of $|m_s|$ are separated by a zero-field splitting of $\omega_0/2\pi \simeq 2.88$ GHz, which originates from nonaveraged spin-spin interactions.[11] For moderate applied magnetic fields,[16] $|\mu_B \vec{B}| \ll \hbar\omega_0$, static and low-frequency components of magnetic fields cause Zeeman shifts of states $|\pm 1\rangle$ while microwave (mw) fields drive Rabi oscillations between $|0\rangle$ and the exited states $|\pm 1\rangle$ as shown in Fig. 2(a). In a frame rotating with the mw frequencies,

$$H_{\rm NV} = \sum_{i=\pm 1} -\hbar\Delta_i |i\rangle\langle i| + \frac{\hbar\Omega_i}{2}(|0\rangle\langle i| + |i\rangle\langle 0|), \qquad (2)$$

where $\Delta_\pm$ and $\Omega_\pm$ denote the detunings and the Rabi frequencies of the two mw transitions. For simplicity we restrict the following discussion to symmetric conditions; i.e., $\Delta_i \equiv \Delta$ and $\Omega_i \equiv \Omega$ (e.g., using a single mw field polarized in x direction and $B_z \to 0$). Hamiltonian (2) then couples the state $|0\rangle$ to a "bright" superposition of excited states $|b\rangle = (|-1\rangle + |+1\rangle)/\sqrt{2}$, while the "dark" superposition $|d\rangle = (|-1\rangle - |+1\rangle)/\sqrt{2}$ remains decoupled. The resulting eigenbasis of $H_{\rm NV}$ is therefore given by $|d\rangle$ and the two dressed states $|g\rangle = \cos(\theta)|0\rangle - \sin(\theta)|b\rangle$ and $|e\rangle = \cos(\theta)|b\rangle + \sin(\theta)|0\rangle$, with $\tan(2\theta) = -\sqrt{2}\Omega/\Delta$. Corresponding eigenfrequencies are $\omega_d = -\Delta$ and $\omega_{e/g} = (-\Delta \pm \sqrt{\Delta^2 + 2\Omega^2})/2$. We will mainly focus on the regime $\Delta < 0$ where $|g\rangle$ is the lowest-energy state [Fig. 2(b)].

To achieve a resonant coupling, values for Ω and $|\Delta|$ can now be adjusted such that transition frequencies between dressed states, e.g., $\omega_{dg} = \omega_d - \omega_g$, become comparable with the oscillator frequency ω_r. Rewriting Hamiltonian (1) in terms of $|g\rangle$, $|d\rangle$, and $|e\rangle$ we obtain

$$H_S = \hbar\omega_r a^\dagger a + \hbar\omega_{eg}|e\rangle\langle e| + \hbar\omega_{dg}|d\rangle\langle d| + \hbar(\lambda_g|g\rangle\langle d| + \lambda_e|d\rangle \times \langle e| + \text{H.c.})(a + a^\dagger), \qquad (3)$$

where $\lambda_g = -\lambda \sin(\theta)$ and $\lambda_e = \lambda \cos(\theta)$. Under resonance conditions, $\omega_r \approx \omega_{gd} \neq \omega_{ed}$ Hamiltonian (3) reduces to the well-known Jaynes-Cummings (JC) model and describes coherent oscillations between states $|n\rangle|g\rangle$ and $|n-1\rangle|d\rangle$, where $|n\rangle$ denotes a phonon number state. To observe the coherent dynamics associated with this model the vacuum Rabi frequency λ_g must be compared to the motional decoherence rate Γ_r and random shifts of the transition frequency, $\Delta\omega_{dg}$, due to hyperfine interactions with the nuclear-spin bath. The condition $\lambda_g > \Gamma_r, \Delta\omega_{dg}$ then defines the strong-coupling regime. While in principle $\Gamma_r \equiv \gamma$ at zero temperature, we identify below $\Gamma_r \equiv k_B T/\hbar Q$ as the relevant decoherence rate for experimentally accessible temperatures T. Interactions with the nuclear-spin bath are characterized by a typical strength $\delta_n \sim 1/T_2^* \sim 1$ MHz which exceeds λ.

To show how the strong-coupling regime can be achieved, we now study the driven NV center in the presence of hyperfine interactions, $H_{\rm nuc} = g_s \mu_B B_{n,z}(t) S_z$, where $\vec{B}_n(t)$ is the effective magnetic field associated with the nuclear-spin bath. $\vec{B}_n(t)$ is quasistatic on the timescales of interest[16] but has a random magnitude on the order of $|B_{n,z}| = \hbar\delta_n/(g_s\mu_B)$. In Fig. 2(c) we plot dressed state energies of $H'_{\rm NV} = H_{\rm NV} + H_{\rm nuc}$ as a function of δ_n. For $\Omega \to 0$ we recover the linear Zeeman shift for the bare spin states $|\pm 1\rangle$. In this regime large random shifts of ω_{dg} would prevent resonant interactions between the spin and the resonator mode. However, for $\Omega \sim |\Delta|$ where the operator S_z has only off-diagonal matrix elements in the dressed state basis, perturbations are suppressed for $\Omega \gg |\delta_n|$. In particular, the quadratic shift of the transition frequency ω_{dg} is given by

$$\Delta\omega_{dg}^{(2)} = \delta_n^2/\omega_{gd}[1 - \tan^{-2}(\theta) + \sin^2(\theta)]. \qquad (4)$$

We find that in the present three-level configuration not only can we eliminate linear shifts of the transition frequency but at a particular value of $\theta \approx \theta_0 \simeq 0.22\pi$ even quadratic corrections vanish. At this "sweet spot" the remaining frequency shift is $\Delta\omega_{gd}^{(4)} \approx 0.6 \times \delta_n^4/\omega_{gd}^3$. In other words, operation at the sweet spot allows us to suppress the effect of $H_{\rm nuc}$ by several orders of magnitude and to treat remaining corrections as a small perturbation.

II. EXAMPLE

As an example we consider a Si cantilever[5] of dimensions $(l, w, t) = (3, 0.05, 0.05)$ μm with a fundamental frequency of $\omega_r/2\pi \approx 7$ MHz and $a_0 \approx 5 \times 10^{-13}$ m. A magnetic tip with size of ~ 100 nm and homogeneous magnetization $M \approx 2.3 \times 10^6$ T/μ_0 (Ref. 6) produces a magnetic gradient of $G_m \approx 7.8 \times 10^6$ T/m at a distance $h \approx 25$ nm away from the tip and results in a coupling strength $\lambda/2\pi \approx 115$ kHz. For a temperature of $T = 100$ mK and Q values of 10^5 the heating rate is $\Gamma_r/2\pi \approx 20$ kHz. Operating close to the sweet spot $\theta \approx \theta_0$ and assuming $\delta_n \simeq 1$ MHz we obtain $(\lambda_g, \Gamma_r, \Delta\omega_{gd}) = 2\pi \times (70, 20, 2)$ kHz. Hence, this combination enables us to access the strong-coupling regime of Hamiltonian (3). For higher values of $Q \sim 10^6$ and/or a reduction in the system dimensions to $h \sim 10$ nm the strong-coupling regime can then be reached even at temperatures up to a few kelvins.

III. APPLICATIONS

Hamiltonian (3) allows a coherent transfer of quantum states between the spin and the resonator modes, which in combination with optical pumping and readout techniques for spin states[12] provides the basic ingredients for the generation and detection of various nonclassical states of the mechanical resonator. Here we discuss in more detail an optical cooling scheme for ground-state preparation and a general strategy for the generation of arbitrary superpositions of resonator states.

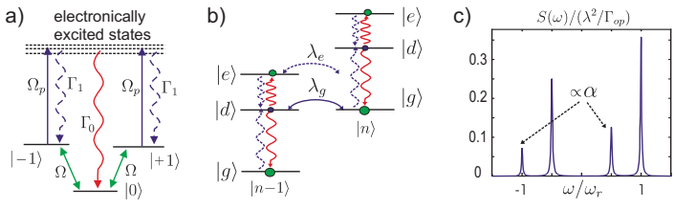

FIG. 3. (Color online) (a) Optical pumping of spin states. (b) Level diagram of Hamiltonian H_S [Eq. (3)]. Wavy lines indicate optical pumping processes into and out of state $|d\rangle$ for $\alpha=0$ (solid line) and $\alpha>0$ (solid and dashed lines). (c) Excitation spectrum $S(\omega)$ [Eq. (6)] for $\omega_{dg}=\omega_r$, $\omega_{ed}\simeq 0.53\omega_r$, and $\Gamma_{\rm op}/\omega_r=0.01$ and $\alpha=1$.

Cooling and state preparation techniques rely on a controlled dissipation of energy which in the present setting can be achieved by optical pumping of spin states as shown in Fig. 3(a). A laser excites spin states $|\pm1\rangle$ into higher electronic levels from where they decay with a rate Γ_1 back to the same spin state or with a rate Γ_0 to state $|0\rangle$. Projected on the electronic ground state we can characterize the pumping process by a tunable pumping rate $\Gamma_{\rm op}(t)=\Omega_p^2(t)\Gamma_0/(\Gamma_1+\Gamma_0)^2$ between states $|\pm1\rangle$ and $|0\rangle$ and the branching ratio $\alpha=\Gamma_1/\Gamma_0$. While off-resonant excitations at room temperature yield $\alpha\sim1$, the ideal limit $\alpha\to0$ can be reached using resonant excitations of appropriately chosen transitions at lower temperatures.[17] Including mechanical dissipation of the resonator mode, the evolution of the system density operator $\rho(t)$ is described by the master equation

$$\dot\rho(t)=i[\rho(t),H_S]+\gamma\{(N_{\rm th}+1)\mathcal{D}[a]+N_{\rm th}\mathcal{D}[a^\dagger]\}\rho+\Gamma_{\rm op}(t)\sum_{i=\pm1}(\mathcal{D}[|0\rangle\langle i|]+\alpha\mathcal{D}[|i\rangle\langle i|])\rho. \quad (5)$$

Here $\mathcal{D}[\hat c]\rho:=(2\hat c\rho\hat c^\dagger-\hat c^\dagger\hat c\rho-\rho\hat c^\dagger\hat c)/2$ and $N_{\rm th}=[\exp(\hbar\omega_r/k_BT)-1]^{-1}$ are the thermal equilibrium occupation number for a support temperature T.

To remove thermal excitations we first study cw cooling of the resonator mode. Assuming $\Gamma_{\rm op}(t)\equiv\Gamma_{\rm op}\gg\lambda$ we eliminate the fast dynamics of the spin degrees of freedom[18] and study the effective evolution of the mean occupation number $\langle n\rangle(t)={\rm Tr}\{\rho(t)a^\dagger a\}$. The resulting equation is of the form $\langle\dot n\rangle=-W(\langle n\rangle-\langle n\rangle_0)$, with a total cooling rate $W=W_{\rm op}+\gamma$ and a final occupation number $\langle n\rangle_0=(\gamma N_{\rm th}+A_{\rm op}^+)/W$. Here the optical cooling and heating rates, $W_{\rm op}=S(\omega_r)-S(-\omega_r)$ and $A_{\rm op}^+=S(-\omega_r)$, are determined by the fluctuation spectrum

$$S(\omega)=2\lambda^2\,{\rm Re}\int_0^\infty d\tau\langle S_z(\tau)S_z\rangle_0 e^{i\omega\tau}, \quad (6)$$

which describes the ability of the spin to absorb ($\omega>0$) or emit ($\omega<0$) a phonon of frequency ω. To achieve ground-state cooling $W_{\rm op}\sim\mathcal{O}(\lambda^2/\Gamma_{\rm op})$ must exceed $A_{\rm op}^+$ *and* the thermal heating rate $\Gamma_r=\gamma N_{\rm th}$, where $\Gamma_r\simeq k_BT/\hbar Q$ for relevant temperatures $k_BT\gg\hbar\omega_r$.

The spectrum $S(\omega)$ is plotted in Fig. 3 for the sideband resolved regime $\lambda<\Gamma_{\rm op}\ll\Omega,|\Delta|,\omega_r$ where individual resonances of width $\sim\Gamma_{\rm op}$ can be assigned to transitions in the level diagram shown in Fig. 3(b). Under resonance conditions, $\omega_r=\omega_{dg}$, cooling is dominated by transitions $|n\rangle|g\rangle\to|n-1\rangle|d\rangle$ corresponding to the peak in the spectrum at $\omega\approx\omega_r$. This cooling process is partially compensated for by heating transitions which can occur for nonzero populations ρ_{ee} and ρ_{dd} of excited states $|e\rangle$ and $|d\rangle$. While $\rho_{ee}\sim1/2$ under strong driving conditions, transitions $|n\rangle|e\rangle\to|n+1\rangle|d\rangle$ are detuned from resonance by $|\omega_{dg}-\omega_{ed}|=|\Delta|$ and do not significantly contribute to heating. The remaining resonant heating process, $|n\rangle|d\rangle\to|n+1\rangle|g\rangle$, is proportional to the occupation of the dark state, which is populated only by optical dephasing processes. Independent of Ω we obtain $\rho_{dd}\propto\alpha$ such that in the limit of ideal optical pumping $\alpha\to0$, the dark state $|d\rangle$ remains unoccupied, thus enabling ground-state cooling with a strongly driven spin.

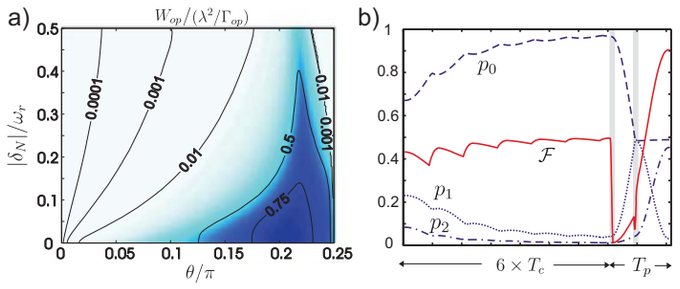

FIG. 4. (Color online) (a) Optical cooling rate $W_{\rm op}$ in the presence of a perturbation $H_{\rm nuc}=\hbar\delta_N S_z$ for $\alpha=0$ and $\Gamma_{\rm op}/\omega_r=0.03$. (b) Preparation of a superposition state $|\psi\rangle$ as discussed in the text where $\mathcal{F}={\rm Tr}\{|\psi\rangle\langle\psi|\rho(t)\}$ and $p_i={\rm Tr}\{|i\rangle\langle i|\rho(t)\}$. The sequence consists of six cooling cycles of duration $T_c\simeq\pi/4\lambda_g+2.5/\Gamma_{\rm op}$ followed by a state preparation stage with $T_p\simeq\pi/(4\lambda_g)+\pi/(\sqrt{8}\lambda_g)$. Gray bars indicate short $\pi/2$ rotations between states $|g\rangle$ and $|d\rangle$. The parameters used for this plot are $\Gamma_r/\lambda_g=0.01$, $\lambda_g/\omega_r=0.01$ and $\Gamma_{\rm op}/\omega_r=0.05$.

We derive analytic expressions for $S(\omega)$ using the quantum regression theorem. To ensure resonance conditions we choose values for $\Delta<0$ and Ω which fulfill $\sqrt{\Delta^2+\Omega^2}=\omega_r/\cos^2(\theta)$ and study cooling as a function of the remaining free parameter $\theta\in[0,\pi/4]$. For $\Delta\omega_{dg}=0$ and $\Gamma_{\rm op}\ll\omega_r$ we then obtain $W_{\rm op}=(\lambda^2/\Gamma_{\rm op})\mathcal{W}$ where

$$\mathcal{W}=\frac{8\cos^4(\theta)\sin^2(\theta)}{[(1+\alpha)+\sin^2(\theta)][1+\cos^2(2\theta)+3\alpha\sin^2(2\theta)/4]}. \quad (7)$$

This function is maximized for $\theta\approx0.2\pi$, and for $\alpha\to0$ we obtain an optimized damping rate of $W_{\rm op}\simeq0.8\times\lambda^2/\Gamma_{\rm op}$. In the presence of hyperfine interactions cooling is suppressed when the level shift $\Delta\omega_{dg}$ exceeds $\Gamma_{\rm op}$. From a numerical evaluation of $W_{\rm op}$ shown in Fig. 4(a) we find that close to $\theta\approx\theta_0$ not only do we optimize $W_{\rm op}$ but cooling is also most insensitive to perturbations. For given $W_{\rm op}\gg\gamma$ the final occupation number is

$$\langle n\rangle_0\simeq\frac{\alpha}{2}\tan^2(\theta)+\frac{1}{Q}\frac{k_BT}{\hbar W_{\rm op}}. \quad (8)$$

By choosing $\Gamma_{\rm op}\sim\lambda$ and $\alpha\approx0$ we find that conditions for ground-state cooling coincide with the strong-coupling regime. Therefore, a single electronic spin can be used to op-

tically cool the resonator into the quantum regime starting from initial temperatures $T \sim 0.1-1$ K. For $\alpha \neq 0$ the apparent intrinsic limit for the present cooling scheme, $\langle n_0 \rangle \sim \alpha/2$, can be overcome by employing a pulsed pumping strategy as discussed below.

Once prepared near its ground state, the resonator state can be completely controlled via Hamiltonian (3). The key mechanism that enables such a control involves the unitary evolution under resonant JC Hamiltonian (3) when $\omega_r = \omega_{dg}$. Specifically, for a time $t = \pi/2\lambda_g$ this evolution maps arbitrary spin states onto superpositions of motional states with zero and one phonon. This procedure can be generalized for the generation of arbitrary states of the form $|\psi\rangle = \Sigma_{n=0}^{M} c_n |n\rangle|g\rangle$ as proposed by Law and Eberly.[19] The basic idea is that we can construct a unitary transformation U such that $U|\psi\rangle = |0\rangle$. Specifically, $|\psi\rangle$ can be coherently mapped to a state $|\psi'\rangle$ with the maximal phonon number reduced by one after a free evolution $U_{\mathrm{JC}}(\tau) = \exp(-iH_S\tau/\hbar)$ followed by a unitary rotation $U_x(\beta) = \exp[-i(\beta|d\rangle\langle g| + \beta^*|g\rangle\langle d|)]$, which can be implemented by an additional external microwave pulse. For appropriately chosen parameters τ and β this combination removes first all population from state $|M\rangle|g\rangle$ and successively from state $|M-1,d\rangle$. By iterating this procedure one can step by step construct a unitary evolution U which maps $|\psi\rangle$ onto the ground state $|0,g\rangle$. Then, by starting from $|0,g\rangle$ the inverse operation U^{-1} will generate the target state $|\psi\rangle = U^{-1}|0,g\rangle$. For a given M the state $|\psi\rangle$ can be generated within a time $t_M \leq M/2\lambda_g$ and a fidelity $\mathcal{F} \simeq (1 - M\pi\Gamma_r/2\lambda_g) \times p_0$, where p_0 is the initial occupation of state $|0,g\rangle$.

As an example of this procedure, we consider the generation of the state $|\psi\rangle = (|0\rangle - |2\rangle)|g\rangle/\sqrt{2}$ starting from a precooled thermal state with $\langle n \rangle = 0.5$. To prepare the initial state $|0,g\rangle$ with high fidelity, independent of α, we use a pulsed pumping scheme. First, with $\Omega(t) = 0$ the spin is optically pumped into the bare spin state $|0\rangle$. In the second step $\Omega(t)$ is turned on adiabatically such that the spin is prepared in state $|g\rangle$ while $|d\rangle$ and $|e\rangle$ remain unoccupied. Finally, for a time $t_{\mathrm{int}} = \pi/(4\lambda_g)$ the system undergoes an oscillation between states $|n\rangle|g\rangle$ and $|n-1\rangle|d\rangle$. The repetition of this pulse sequence successively removes motional excitations and prepares the resonator in the state $|0,g\rangle$ with a probability $p_0 \simeq 1 - (\pi\Gamma_r/4\lambda_g)$. Next, a sequence of two mw pulses and two partial swaps is used to prepare the catlike state $(|0\rangle - |2\rangle)/\sqrt{2}$. Figure 4 shows the results of a numerical integration of master equation (5) simulating six cooling cycles followed by the state preparation sequence. This example demonstrates that quantum "engineering" of motional states is possible using the present technique. Finally, the mapping procedure can be used for spin-mediated readout of the mechanical motional states.

In summary, we have shown that a single electronic spin qubit in diamond can be strongly coupled to the motion of a nanomechanical resonator. Such a strong coupling enables ground-state cooling and quantum-by-quantum generation of arbitrary states of the resonator mode. Potential applications include the use of nonclassical motional states for improved antiferromagetic-based force and magnetic sensing techniques,[5] as well as for tests of fundamental theories.[4]

ACKNOWLEDGMENTS

We thank M. Aspelmeyer, A. Yacoby, P. Zoller, and W. Zwerger for stimulating discussions. This work was supported by the ITAMP, the NSF, and the Packard Foundation.

[1] J. Eisert, M. B. Plenio, S. Bose, and J. Hartley, Phys. Rev. Lett. **93**, 190402 (2004).

[2] D. Vitali, S. Gigan, A. Ferreira, H. R. Böhm, P. Tombesi, A. Guerreiro, V. Vedral, A. Zeilinger, and M. Aspelmeyer, Phys. Rev. Lett. **98**, 030405 (2007).

[3] A. D. Armour, M. P. Blencowe, and K. C. Schwab, Phys. Rev. Lett. **88**, 148301 (2002).

[4] W. Marshall, C. Simon, R. Penrose, and D. Bouwmeester, Phys. Rev. Lett. **91**, 130401 (2003).

[5] J. A. Sidles, J. L. Garbini, K. J. Bruland, D. Rugar, O. Züger, S. Hoen, and C. S. Yannoni, Rev. Mod. Phys. **67**, 249 (1995).

[6] H. J. Mamin, M. Poggio, C. L. Degen, and D. Rugar, Nat. Nanotechnol. **2**, 301 (2007).

[7] C. H. Metzger and K. Karrai, Nature **432**, 1002 (2004); S. Gigan *et al.*, *ibid.* **444**, 67 (2006); O. Arcizet *et al.*, *ibid.* **444**, 71 (2006); D. Kleckner and D. Bouwmeester, *ibid.* **444**, 75 (2006); T. Corbitt, C. Wipf, T. Bodiya, D. Ottaway, D. Sigg, N. Smith, S. Whitcomb, and N. Mavalvala, Phys. Rev. Lett. **99**, 160801 (2007); J. D. Thompson *et al.*, Nature (London) **452**, 72 (2008); A. Schliesser *et al.*, Nat. Phys. **4**, 415 (2008).

[8] A. Naik, O. Buu, M. D. LaHaye, A. D. Armour, A. A. Clerk, M. P. Blencowe, and K. C. Schwab, Nature (London) **443**, 193 (2006).

[9] J. D. Teufel, J. W. Harlow, C. A. Regal, and K. W. Lehnert, Phys. Rev. Lett. **101**, 197203 (2008).

[10] P. Treutlein, D. Hunger, S. Camerer, T. W. Hänsch, and Jakob Reichel, Phys. Rev. Lett. **99**, 140403 (2007).

[11] J. Wrachtrup and F. Jelezko, J. Phys.: Condens. Matter **18**, S807 (2006).

[12] R. Hanson, F. M. Mendoza, R. J. Epstein, and D. D. Awschalom, Phys. Rev. Lett. **97**, 087601 (2006); L. Childress *et al.*, Science **314**, 281 (2006); T. Gaebel *et al.*, Nat. Phys. **2**, 408 (2006).

[13] J. M. Taylor *et al.*, Nat. Phys. **4**, 810 (2008); C. L. Degen, Appl. Phys. Lett. **92**, 243111 (2008).

[14] J. R. Maze *et al.*, Nature (London) **455**, 644 (2008); G. Balasubramanian *et al.*, *ibid.* **455**, 648 (2008).

[15] I. Wilson-Rae, P. Zoller, and A. Imamoglu, Phys. Rev. Lett. **92**, 075507 (2004).

[16] This assumes that in the vicinity of the NV center static magnetic fields from the tip are canceled by an external bias field $\vec{B}_{\mathrm{bias}}$.

[17] See, for example, P. Tamarat *et al.*, New J. Phys. **10**, 045004 (2008) and references therein.

[18] J. I. Cirac, R. Blatt, P. Zoller, and W. D. Phillips, Phys. Rev. A **46**, 2668 (1992).

[19] C. K. Law and J. H. Eberly, Phys. Rev. Lett. **76**, 1055 (1996).